Acta Crystallographica Section B
Structural Science
ISSN 0108-7681

X-ray crystallographic structures of enamine and amine Schiff bases of pyridoxal and its 1:1 hydrogen-bonded complexes with benzoic acid derivatives: evidence for coupled inter- and intramolecular proton transfer

Shasad Sharif,[a] Douglas R. Powell,[b] David Schagen,[a] Thomas Steiner,[c] Michael D. Toney,[d] Emily Fogle[d] and Hans-Heinrich Limbach[a]*

[a]Institut für Chemie, Freie Universität Berlin, Takustrasse 3, D-14195 Berlin, Germany, [b]Department of Chemistry, University of Kansas, Lawrence, KS 66045-7582, USA, [c]Institut für Chemie-Kristallographie, Freie Universität Berlin, Takustrasse 6, D-14195 Berlin, Germany, and [d]Department of Chemistry, University of California–Davis, Davis, CA 95616, USA

Correspondence e-mail: limbach@chemie.fu-berlin.de

Received 10 September 2005
Accepted 5 December 2005

Crystal structures of Schiff bases containing pyridoxal (PL), *N*-(pyridoxylidene)-tolylamine, $C_{15}H_{16}N_2O_2$ (I), *N*-(pyridoxylidene)-methylamine, $C_9H_{12}N_2O_2$ (III), and their 1:1 adduct with 2-nitrobenzoic acid, $(I)^+$ $C_7H_4NO_4^-$ (II), and 4-nitrobenzoic acid, $(III)^+$ $C_7H_4NO_4^-$ (IV), serve as models for the coenzyme pyridoxal-5′-phosphate (PLP) in its PLP-dependent enzymes. These models allow the study of the intramolecular OHN hydrogen bond of PL/PLP Schiff bases and the H-acceptor properties of their pyridine rings. The free base (I) forms hydrogen-bonded chains involving the hydroxyl side groups and the rings of adjacent molecules, whereas (III) forms related hydrogen-bonded cyclic dimers. The adducts (II)/(IV) consist of 1:1 hydrogen-bonded complexes, exhibiting strong intermolecular bonds between the carboxylic groups of the acids and the pyridine rings of (I)/(III). In conclusion, the proton in the intramolecular O—H···N hydrogen bond of (I)/(III) is located close to oxygen (enolamine form). The added acids protonate the pyridine ring in (II)/(IV), but only in the latter case does this protonation lead to a shift of the intramolecular proton towards the nitrogen (ketoimine form). All crystallographic structures were observed in the *open form*. In contrast, the formation of the pyridinium salt by dissolving (IV) leads to the *cyclic aminal* form.

1. Introduction

In various enzymatic transformations of amino acids (*e.g.* racemization, decarboxylation and transamination), the cofactor (vitamin B6) pyridoxal-5′-phosphate (PLP; Christen & Metzler, 1985; Fujiwara, 1973) plays an important role (Malashkevich *et al.*, 1993; Spies & Toney, 2003; Zhou & Toney, 1999). According to the crystal structures of PLP-dependent enzymes (Jansonius, 1998; Jager *et al.*, 1994; Shaw *et al.*, 1997; Smith *et al.*, 1989; Stamper *et al.*, 1998), the cofactor is tightly bound at their active sites (Fig. 1*d*). The ring nitrogen is involved in an intermolecular OHN hydrogen bond with an aspartic acid side-chain and the phosphate group forms three hydrogen bonds with other amino acid residues. Whereas in aqueous solution the aldehyde function of PLP is easily hydrated (Harruff & Jenkins, 1976; van Genderen *et al.*, 1989; Witherup & Abbott, 1975), PLP forms in the enzymatic environment in the absence of the substrate generally a so-called ‘internal aldimine’, consisting of a Schiff base with the ε-amino group of a lysine residue of the enzyme. ‘External aldimines’ are formed with the amino acid substrates and their

reaction products. The aldehyde and all aldimines contain an additional intramolecular hydrogen bond that is essential for the enzymatic function (Christen & Metzler, 1985).

Of special importance are two functional OHN hydrogen bonds, as illustrated below. In the first step of the catalytic cycle (Fig. 2), it is assumed that the bridging proton of the intramolecular O···H—N hydrogen bond has to be transferred from the hydroxyl oxygen to the imino nitrogen, a process that is assisted by the protonation of the pyridine ring. The role of the intermolecular O···H—N hydrogen bond is not clear: it could first serve as an attachment point of the cofactor with the protein, as the phosphate group, but it could also assist the proton transfer in the intramolecular O···H—N hydrogen bond.

In order to elucidate the role of the intramolecular hydrogen bond, model studies have been reported for several model Schiff bases of aromatic *ortho*-hydroxylaldehydes, dissolved in organic liquids or embedded in the organic solid state (Benedict *et al.*, 1998; Dziembowska *et al.*, 2001; Hansen *et al.*, 1998; Limbach *et al.*, 2004; Rozwadowski *et al.*, 1999). In these studies, the existence of tautomeric equilibria between enolimine (OH) forms and ketoamine (NH) forms that interconvert has been established interconverting very rapidly *via* proton transfers (Fig. 3). As these models did not contain the pyridine ring function or the phosphate group, the influence of these substitutents on the intramolecular hydrogen bond was not studied.

Therefore, we have been interested in the coupling of the intra- and the intermolecular OHN hydrogen bonds, a problem that we wanted to study by a combination of crystallographic and liquid-state NMR techniques. However, for this task it was necessary to design and crystallize model Schiff bases that mimic the PLP cofactor in its natural environment.

As the phosphate group is not directly involved in the chemical function of PLP, we prepared several novel 1:1 acid–base complexes of benzoic acid derivatives with Schiff bases of pyridoxal (PL, R' = H, see Fig. 1*a*; MacLaurin & Richardson, 1985), with R = tolyl and methyl, in order to vary the basicity of the Schiff base N atom. We were able to crystallize compounds (I) to (IV) depicted in Fig. 4, whose X-ray crystallographic structures are reported in this paper. We note that we have searched without success in the Cambridge Structural Database (CSD) for other examples of Schiff bases containing PLP or PL, which can mimic the coupling of the intra- and intermolecular hydrogen bonds.

2. Experimental

^{1}H NMR in the liquid state was recorded at 500.13 MHz in dimethylsulfoxide-d_6 (d_6-DMSO) at room temperature. The ^{1}H spectra were referenced to TMS using the dimethylsulfoxide-d_6 (2.49 p.p.m.) signal as the internal reference; the proton recycle time was 2 s. Multiplicities are as follows: s, singlet; d, doublet; t, triplet; m, multiplet. The assignment of the NMR peaks of the free Schiff bases (I) was compared with the PL skeleton (Christen & Metzler, 1985; Harruff & Jenkins, 1976; Witherup & Abbott, 1975); (III) refers to van Genderen *et al.* (1989); the acid–base adducts (II) and (IV) were compared with the ^{1}H spectra of the free benzoic acid derivatives and Schiff bases. The compounds synthesized were characterized by X-ray crystallography as reported above, but also by elemental analysis and NMR in solution.

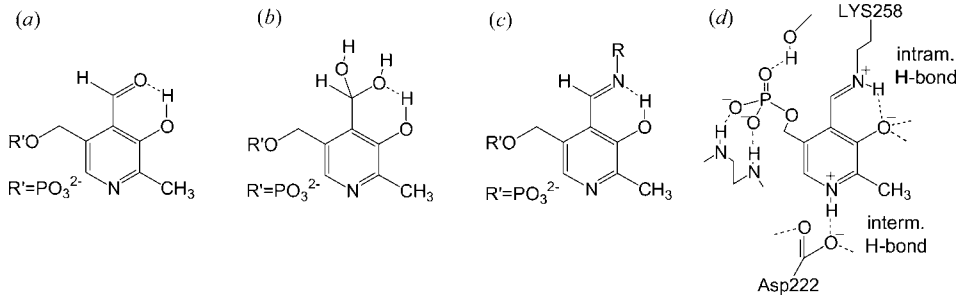

Figure 1
(*a*) PLP aldehyde form. (*b*) PLP hydrate form. (*c*) PLP Schiff base. (*d*) PLP 'internal aldimine'.

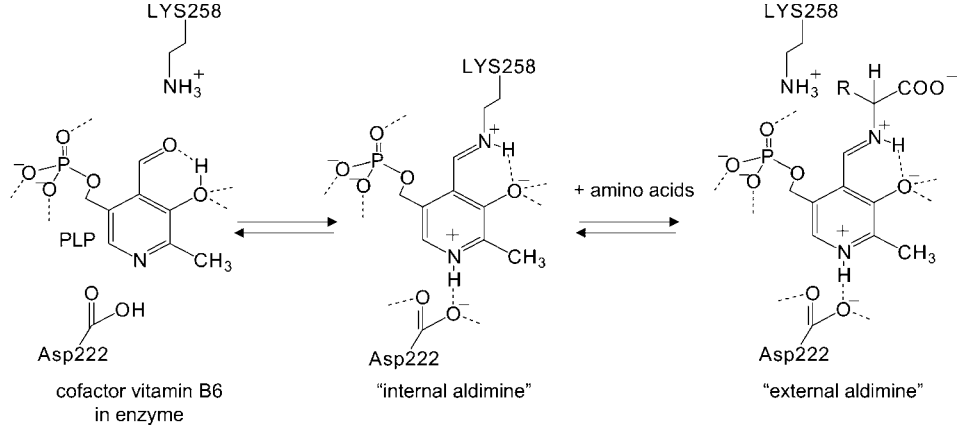

Figure 2
Overview of the first step of the catalytic cycle.

2.1. X-ray structure determination

Data were collected on a Stoe four-circle diffractometer for (I) and (II), and on a Bruker Apex diffractometer equipped with a CCD area detector for (II) and

Table 1
Crystallographic data of the Schiff bases and their 1:1 adducts with benzoic acid derivatives.

	(I)	(II)	(III)	(IV)
Crystal data				
Chemical formula	$C_{15}H_{16}N_2O_2$	$C_{15}H_{17}N_2O_2{\cdot}C_7H_4NO_4$	$C_9H_{12}N_2O_2$	$C_9H_{13}N_2O_2{\cdot}C_7H_4NO_4$
M_r	256.30	423.42	180.21	347.33
Cell setting, space group	Monoclinic, $P2_1/n$	Triclinic, $P\overline{1}$	Monoclinic, $P2_1/c$	Monoclinic, $P2_1/c$
a, b, c (Å)	4.001 (4), 25.09 (3), 12.940 (11)	7.683 (5), 12.188 (6), 12.562 (6)	11.046 (2), 4.8739 (8), 18.027 (3)	7.113 (2), 11.797 (3), 18.314 (5)
α, β, γ (°)	90.00, 93.65 (8), 90.00	114.88 (4), 99.61 (5), 96.03 (5)	90.00, 106.728 (5), 90.00	90.00, 94.644 (7), 90.00
V (Å^3)	1296 (2)	1031.8 (10)	929.5 (3)	1531.7 (7)
Z	4	2	4	4
D_x (Mg m^{-3})	1.313	1.363	1.288	1.506
Radiation type	Mo $K\alpha$	Mo $K\alpha$	Mo $K\alpha$	Mo $K\alpha$
No. of reflections for cell parameters	25	25	2559	5759
θ range (°)	8.0–15.0	7.0–15.0	2.3–26.0	2.2–26.0
μ (mm^{-1})	0.09	0.10	0.09	0.12
Temperature (K)	295 (2)	295 (2)	295 (2)	100 (2)
Crystal form, color	Plate, yellow	Plate, yellow	Prism, yellow	Plate, yellow
Crystal size (mm)	0.40 × 0.20 × 0.10	0.40 × 0.20 × 0.10	0.45 × 0.23 × 0.04	0.38 × 0.34 × 0.10
Data collection				
Diffractometer	Stoe four-circle	Stoe four-circle	Bruker APEX	Bruker APEX
Data collection method	ω scans	ω scans	ω scans	ω scans
Absorption correction	None	None	Multi-scan (based on symmetry-related measurements)	Multi-scan (based on symmetry-related measurements)
T_{min}	–	–	0.942	0.954
T_{max}	–	–	0.996	0.989
No. of measured, independent and observed reflections	2631, 2287, 874	3866, 3591, 2383	7547, 1814, 1575	13 011, 3005, 2768
Criterion for observed reflections	$I > 2\sigma(I)$	$I > 2\sigma(I)$	$I > 2\sigma(I)$	$I > 2\sigma(I)$
R_{int}	0.150	0.018	0.018	0.027
θ_{max} (°)	25.0	25.0	26.0	26.0
Range of h, k, l	$0 \Rightarrow h \Rightarrow 4$ $-29 \Rightarrow k \Rightarrow 29$ $-15 \Rightarrow l \Rightarrow 14$	$-9 \Rightarrow h \Rightarrow 8$ $-10 \Rightarrow k \Rightarrow 14$ $-14 \Rightarrow l \Rightarrow 14$	$-13 \Rightarrow h \Rightarrow 13$ $-5 \Rightarrow k \Rightarrow 6$ $-22 \Rightarrow l \Rightarrow 22$	$-8 \Rightarrow h \Rightarrow 8$ $-14 \Rightarrow k \Rightarrow 14$ $-22 \Rightarrow l \Rightarrow 22$
No. and frequency of standard reflections	3 every 30 min	3 every 30 min	–	–
Intensity decay (%)	3	3	< 0.1	< 0.1
Refinement				
Refinement on	F^2	F^2	F^2	F^2
$R[F^2 > 2\sigma(F^2)]$, $wR(F^2)$, S	0.076, 0.214, 1.00	0.049, 0.153, 1.00	0.051, 0.147, 1.02	0.036, 0.098, 1.00
No. of reflections	2287	3591	1814	3005
No. of parameters	178	289	124	235
H-atom treatment	Mixture of independent and constrained refinement	Mixture of independent and constrained refinement	Mixture of independent and constrained refinement	Mixture of independent and constrained refinement
Weighting scheme	$w = 1/[\sigma^2(F_o^2) + (0.054P)^2]$, where $P = (F_o^2 + 2F_c^2)/3$	$w = 1/[\sigma^2(F_o^2) + (0.078P)^2 + 0.250P]$, where $P = (F_o^2 + 2F_c^2)/3$	$w = 1/[\sigma^2(F_o^2) + (0.081P)^2 + 0.210P]$, where $P = (F_o^2 + 2F_c^2)/3$	$w = 1/[\sigma^2(F_o^2) + (0.051P)^2 + 0.840P]$, where $P = (F_o^2 + 2F_c^2)/3$
$(\Delta/\sigma)_{max}$	< 0.0001	< 0.0001	< 0.0001	0.001
$\Delta\rho_{max}$, $\Delta\rho_{min}$ (e Å^{-3})	0.19, −0.27	0.20, −0.20	0.20, −0.15	0.27, −0.24

Computer programs used: *SMART*, *SAINT*, *SHELXTL* (Sheldrick, 2000).

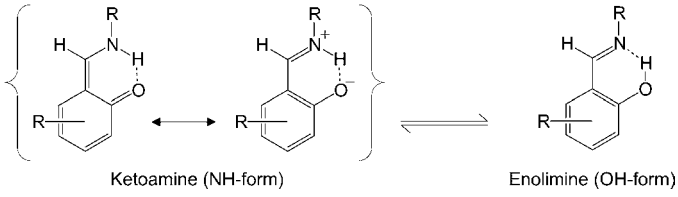

Figure 3
Keto–enol tautomeric equilibrium of the intramolecular hydrogen bond.

(IV), and corrected for absorption using the *SADABS* program (Sheldrick, 2002). Data reduction was performed using Bruker *SMART*, Bruker *SAINT* and *SHELXTL* (Sheldrick, 2000) programs. For details, see Table 1.[1] For (I): R = 0.0752, wR = 0.265, based on 2285 unique reflections

[1] Supplementary data for this paper are available from the IUCr electronic archives (Reference: SN5027). Services for accessing these data are described at the back of the journal.

collected at 295 (2) K and 190 model parameters; for (II): R = 0.0597, wR = 0.1808, based on 4399 unique reflections collected at 295 (2) K and 294 model parameters; for (III): R = 0.0508, wR = 0.1474, based on 1575 unique reflections collected at 295 (2) K and 118 model parameters; (IV): $R1$ = 0.0371, $wR2$ = 0.0991, based on 2768 unique reflections collected at 100 (2) K and 226 model parameters. The positions of H atoms bonded to C atoms were determined by geometry and their positions were refined using a riding model. H atoms bonded to N and O atoms were located from a difference map, and their positions were refined independently.

2.2. Crystallization and synthesis

In this paragraph the synthesis of (I)–(IV) as well as details of the preparations of the crystals are described.

2.2.1. Compound (I). *N*-(Pyridoxylidene)-tolylamine (I) was prepared using a method descried by Iwanami *et al.* (1968), in which pyridoxal hydrochloride was condensed in aqueous solution at pH 7.5 with *p*-toluidine to the Schiff base (I). Compound (I) was crystallized by dissolving it in excess dichloromethane and slowly evaporating it at room temperature. The crystals were filtered, washed with diethyl ether and dried over potassium hydroxide. M.p. 463–466 K, ^{1}H NMR (500 MHz, DMSO-d_6, 300 K, only in *open form*) δ (p.p.m., TMS) = 2.35 (s, 3H, 1‴-CH_3), 2.42 (s, 3H, 2′-CH_3), 4.76 [d, 2H, ^3J(H,H) = 5.4 Hz, 5′-CH_2-], 5.42 [t, 1H, ^3J(H,H) = 5.4 Hz, 5″-OH], 7.25–7.45 (m, 4H, H2″,3″,5″,6″), 7.97 (s, 1H, H6), 9.17 (s, 1H, H4′), 14.04 (s, 1H, H3′). Analysis calculated for $C_{15}H_{16}N_2O_2$: C 68.49, H 2.39, N 10.93%; found: C 70.18, H 6.36, N 10.98%.

2.2.2. Compound (II). The *N*-(pyridoxylidene)-tolylamine (I)–2-nitrobenzoic acid complex (II) was prepared by adding (I) (1 g, 3.9 mmol) to a solution of 4-nitrobenzoic acid (0.63 g, 3.8 mmol) in dichloromethane. Complex (II) can be crystallized by diluting the solution with dichloromethane and slowly evaporating the solvent under reduced pressure. The crystals were filtered, washed with diethyl ether and dried over potassium hydroxide. M.p. decomposition < 443 K, ^{1}H NMR (500 MHz, DMSO-d_6, 300 K, only in *open form*) δ (p.p.m., TMS) = 2.35 (s, 3H, 1‴-CH_3), 2.42 (s, 3H, 2′-CH_3), 4.76 (s, 2H, 5′-CH_2- broad), 5.40 (s, 1H, 5″-OH broad), 7.25–7.45 (m, 4H, H2″,3″,5″,6″), 7.98 (s, 1H, H6), 9.17 (s, 1H, H4′), 14.04 (s, 1H, H3′ broad) [(I)], 7.7–8.0 (m, 4H, H3*A*,4*A*,5*A*,H6*A*), 9.46 (s, 1H, OH broad) p.p.m. (2-nitrobenzoic acid).

2.2.3. Compound (III). *N*-(Pyridoxylidene)-methylamine (III) was prepared after a method described in the literature (Heyl *et al.*, 1948, 1952; Metzler, 1957; van Genderen *et al.*, 1989), where pyridoxal hydrochloride was condensed in methanolic solution with methylamine hydrochloride to the Schiff base (III). Compound (III) was crystallized from dioxane/hexane (1:4) at room temperature. The crystals were filtered, washed with hexane and dried over potassium hydroxide. M.p. 418–419 K, ^{1}H NMR (500.13 MHz, DMSO-d_6, 300 K, only in *open form*) δ (p.p.m., TMS): 2.35 (s, 3H, 2′-CH_3),

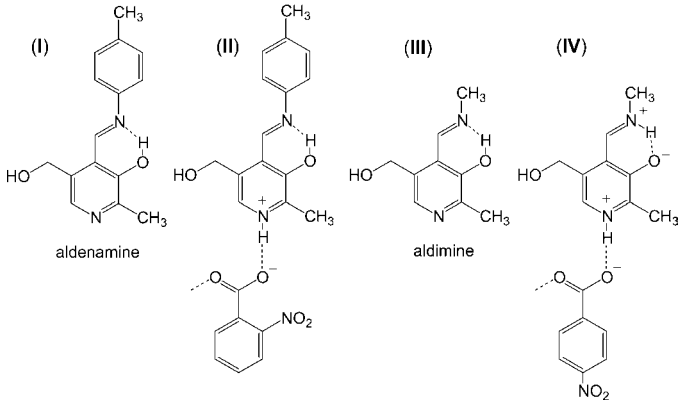

Figure 4
Overview of the structures (I)–(IV).

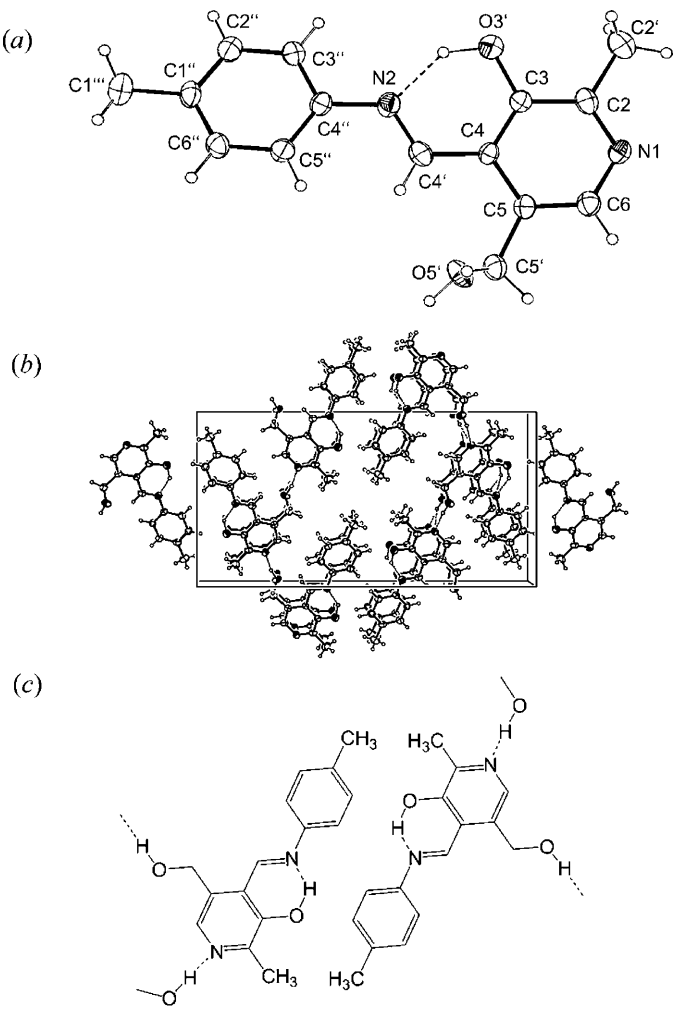

Figure 5
(*a*) X-ray crystal structure of (I) showing the atom-numbering scheme. Displacement ellipsoids are drawn at the 30% probability level. (*b*) Crystal packing of (I) along the *a* axis. (*c*) Showing schematically the formation of pairs of (I) and the molecules which form O—H···N hydrogen bonds involving the hydroxyl side groups and the pyridine rings of adjacent molecules.

Table 2
Selected geometric parameters (Å, °) of (I)–(IV).

		(I)	(II)	(III)	(IV)
Intramolecular hydrogen bond	N2—C4′	1.282 (7)	1.270 (3)	1.263 (2)	1.2922 (18)
	C4′—C4	1.437 (7)	1.450 (3)	1.463 (2)	1.4340 (19)
	C4—C3	1.368 (7)	1.395 (4)	1.399 (2)	1.4334 (19)
	C3—O3′	1.358 (7)	1.337 (3)	1.344 (2)	1.2702 (17)
	N2—C4′—C4	120.4 (6)	121.0 (2)	121.49 (17)	121.92 (12)
	C4′—C4—C3	121.3 (5)	119.8 (3)	120.10 (15)	119.45 (12)
	C4—C3—O3′	122.6 (5)	122.8 (2)	122.27 (16)	123.92 (12)
	C3—C4—C4′—N2	0.1 (9)	−3.8 (4)	2.9 (2)	−0.96 (19)
Intermolecular hydrogen bond	N1—C6	1.351 (7)	1.341 (3)	1.343 (2)	1.3643 (18)
	N1—C2	1.325 (7)	1.322 (3)	1.323 (2)	1.3236 (18)
	C5′—O5′	1.413 (7)	1.410 (3)	1.417 (2)	1.4222 (16)
	C5′—C5	1.504 (7)	1.505 (4)	1.507 (2)	1.5160 (18)
	C6—N1—C2	118.5 (5)	123.3 (2)	118.57 (15)	124.04 (11)
	C5—C5′—O5′	109.7 (5)	112.8 (2)	112.37 (14)	112.59 (11)
	C5′—C5—C6	119.2 (5)	119.7 (2)	119.12 (15)	119.26 (12)
	C6—C5—C5′—O5′	111.6 (6)	−121.9 (3)	104.48 (18)	−117.39 (13)
1:1 adducts	C7*A*—O2*A*		1.256 (3)		1.2603 (17)
	C7*A*—O1*A*		1.228 (3)		1.2517 (18)
	C7*A*—C1*A*		1.508 (3)		1.5201 (19)
	O2*A*—C7*A*—O1*A*		126.4 (2)		125.60 (13)
	O2*A*—C7*A*—C1*A*		114.5 (2)		117.82 (12)
	O1*A*—C7*A*—C1*A*		119.1 (2)		116.58 (12)
	O2*A*—C7*A*—C1*A*—C6*A*		140.8 (2)		20.35 (18)
	O1*A*—C7*A*—C1*A*—C6*A*		−36.6 (4)		−159.08 (13)

Table 3
Hydrogen-bonding parameters (Å, °) of (I)–(IV).

		D—H···*A*	*D*—H	H···*A*	*D*···*A*	< (*D*—H···*A*)
(I)	Intramolecular hydrogen bond	O3′—H3′···N2	1.01 (6)	1.71 (6)	2.545 (6)	138 (5)
	Intermolecular hydrogen bond	O5′—H5′···N1^{i}	0.92 (6)	1.86 (6)	2.752 (7)	162 (5)
(II)	Intramolecular hydrogen bond	O3′—H3′···N2	0.95 (3)	1.69 (3)	2.553 (3)	150 (3)
	Intermolecular hydrogen bond	N1—H1···O2*A*	1.01 (3)	1.55 (3)	2.549 (3)	170 (2)
	Intermolecular hydrogen bond	O5′—H5′···O1*A*^{ii}	0.96 (3)	1.75 (3)	2.704 (3)	175 (3)
(III)	Intramolecular hydrogen bond	O3′—H3′···N2	0.92 (3)	1.73 (3)	2.570 (2)	152 (2)
	Intermolecular hydrogen bond	O5′—H5′···N1^{iii}	0.92 (3)	1.95 (3)	2.865 (2)	171 (2)
(IV)	Intramolecular hydrogen bond	N2—H2···O3′	0.93 (3)	1.81 (2)	2.595 (2)	141 (2)
	Intermolecular hydrogen bond	N1—H1···O2*A*	0.95 (2)	1.71 (2)	2.614 (2)	160 (2)
	Intermolecular hydrogen bond	O5′—H5′···O1*A*^{iv}	0.86 (2)	1.84 (2)	2.700 (2)	175 (2)

3.50 (s, 3H, 4″-CH_3), 4.63 (s, 2H, 5′-CH_2-), 5.32 (s, 1H, broad 5′-CH_2OH), 7.85 (s, 1H, H6), 8.86 (s, 1H, H4′), 14.32 (s, 1H, H3′). Analysis: calculated for $C_9H_{12}N_2O_2$: C 59.98, H 6.72, N 15.55%; found: C 60.55, H 6.57, N 15.15%.

2.2.4. Compound (IV). The *N*-(pyridoxylidene)-methylamine (III)–4-nitrobenzoic acid complex (IV) was prepared by adding (III) (1 g, 5.55 mmol) to a solution of 4-nitrobenzoic acid (0.89 g, 5.32 mmol) in absolute THF. Complex (IV) can be crystallized by two procedures: slowly evaporating the solvent under reduced pressure or stepwise cooling the mixture to 269 K. The crystals were filtered, washed with diethyl ether and dried over potassium hydroxide. M.p. 418–422 K, ^{1}H NMR (500.13 MHz, DMSO-d_6, 300 K) δ (p.p.m., TMS): 2.34 (s, 3H, 2′-CH_3), 3.50 (s, 3H, 4″-CH_3), 4.67 (s, 2H, 5′-CH_2-), 7.84 (s, 1H, H6), 8.86 (s,1H, H4′) of *open form* and 6.18 (s, 1H, H4′), 2.37 (s, 3H, 2′-CH_3), 2.27 (s, 1H, -NH) of *cyclic aminal form* [(III)], 8.15–8.35 (m, 4H, H2*A*, H3*A*, H5*A*, H6*A*), 7.69 (OH, broad, 4-nitrobenzoic acid). Analysis: calculated for $C_{16}H_{17}N_3O_6$: C 55.33, H 4.93, N 12.10%; found: C 55.44, H 4.70, N 11.99%.

3. Results and discussion

The X-ray crystal structures of the known compounds (I) and (III) have not yet been reported in the Cambridge Structural Database (CSD). Unfortunately, it was not possible to crystallize the adducts of (I) and (III) with the same benzoic acid derivative. However, we thought that this would not constitute a major problem as the acidities of 2-nitrobenzoic acid and 4-nitrobenzoic acid, with pK_a = 2.17 and 3.44, respectively (Polanski & Bak, 2003), are not very different. However, owing to the steric hindrance in 2-nitrobenzoic acid being caused by the carboxyl and nitro groups in *ortho* positions, these substituted groups can no longer lie in the plane of the benzene ring, which is not present in 4-nitrobenzoic acid (Kurahashi *et al.*, 1967; Sakore & Pant, 1966).

The structures, crystal packing and the hydrogen-bond network of (I)–(IV) are depicted in Figs. 1–4, selected structural and hydrogen bond data are assembled in Tables 2 and 3. In the following, we will first discuss the hydrogen-bonded networks and the packing diagrams of these crystals, as well as the problem of the location of the protons in the intra- and the intermolecular hydrogen bonds.

The aldenamine Schiff base (I) (Fig. 5) forms O—H···N hydrogen-bonded chains involving the hydroxyl side groups and the pyridine rings of adjacent molecules, exhibiting an N···O distance of the intermolecular hydrogen bond of 2.752 (7) Å (I). It should be mentioned that the chain is excluded by another O—H···N intermolecular hydrogen bond that makes the crystal packing of (I) more complex (Fig. 5). In the intramolecular O—H···N hydrogen bridge the proton is located near the O atom that is supported by the single-bond character of the C3′—O3′ distance of 1.358 (3) Å (I) and the double-bond character of the N2—C4′ distance of 1.2919 (18) Å (I), expected for an enolimine form of the Schiff base. These findings are in agreement with other crystallographic structures where PL is linked as a hydrazone (Domiano *et al.*, 1978; Ferrari *et al.*, 2002; Souron *et al.*, 1995).

In the aldenamine Schiff base–2-nitrobenzoic acid adduct (II) (Fig. 6) the bonding situation in the intramolecular O—H···N hydrogen bond is not altered compared with (I). However, the pyridine ring is now involved in an intermolecular O···H—N hydrogen bond with the carboxylic group of the acid added. The crystal packing shows that the hydroxyl group of the Schiff base is involved in an intermolecular OHO hydrogen bond to the carboxyl group of the acid, in particular to the free oxygen atom O1*A* with the corresponding O···O distance of 2.699 (3) Å. The benzene ring in (II) is not located in the plane of the carboxyl group. The *ortho*-nitro group attached to C2*A* is twisted because of steric hindrance with the neighboring carboxyl group. The bond angles of the benzene ring show significant deviations from 120°, probably because of the presence of the electron-withdrawing nitro and carboxylic groups. These findings are in agreement with earlier X-ray crystallographic studies on complexes of 2,4,6-trimethylpyridine (collidine) with derivatives of benzoic acids (Foces-Foces *et al.*, 1999).

The O···N distance of the intermolecular O···H—N hydrogen bond in (II) is only 2.550 (3) Å. This represents a substantial compression of the heavy atom distance compared with the weaker intermolecular O—H···N hydrogen bonds of (I). The proton is located near to the ring N1 atom leading to a zwitterionic structure. This conclusion is corroborated by the observation that the C2—N1—C6 angle of the pyridine ring increases substantially by protonation of the N atom, and that the two C—O bond lengths of the carboxylic acid groups become equal upon ionization.

The crystal structure of the aldimine Schiff base (III) is depicted in Fig. 7. Although the basicity of the CH_3—N group is expected to be larger than that of the corresponding tolyl-*N* group in (I), the proton in the intramolecular O—H···N hydrogen bond remains on the O atom: the C3′—O3′ distance of 1.342 (2) Å (III) and the N2—C4′ distance of 1.263 (2) Å (III) again suggest an enolimine form. (III) is packed as cyclic centrosymmetric dimers, involving intermolecular O—H···N hydrogen bonds between the hydroxylic side group and the pyridine rings. The N···O distance is

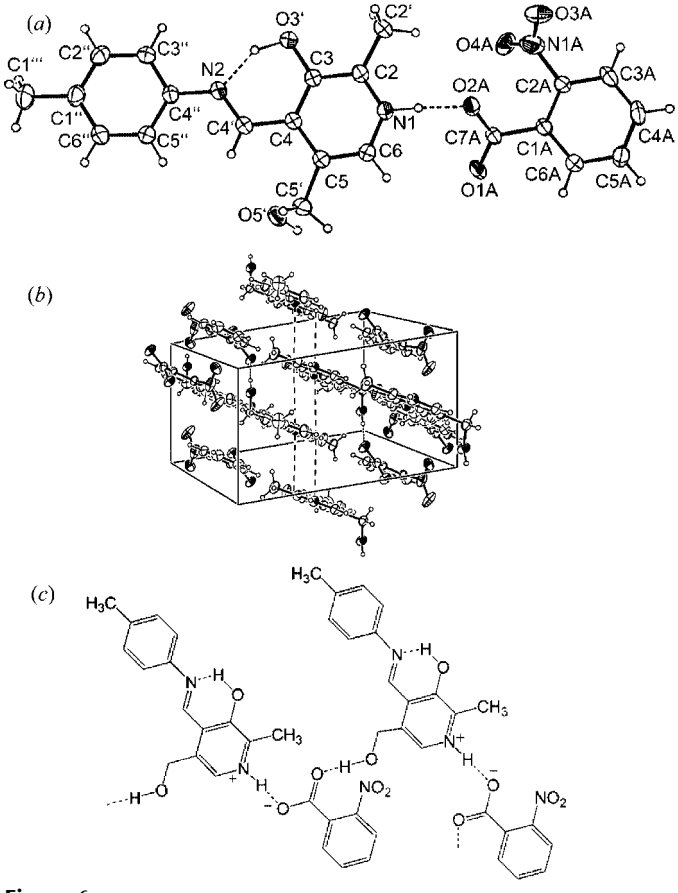

Figure 6
(*a*) X-ray crystal structure of (II) showing the atom-numbering scheme. Displacement ellipsoids are drawn at the 30% probability level. (*b*) Crystal packing of (II) along the *b* axis. (*c*) Showing schematically the stacking in columns of the pairs of molecules (II) and the differences in the packing of these columns.

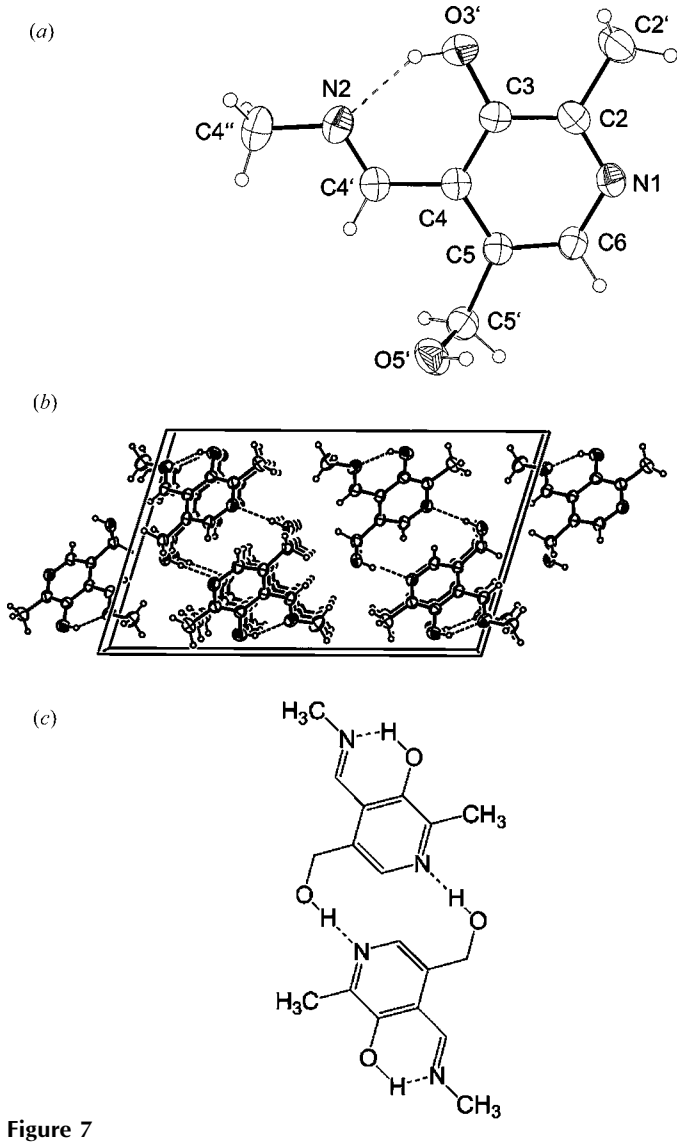

Figure 7
(*a*) X-ray crystal structure of (III) showing the atom-numbering scheme. Displacement ellipsoids are drawn at the 30% probability level. (*b*) Crystal packing of (III) along the *b* axis. (*c*) Showing schematically the formation of centrosymmetric dimers of (III).

2.868 (2) Å, substantially larger than in the corresponding chains of (I).

The crystal structure of the aldimine Schiff base-4-nitrobenzoic acid adduct (IV) is depicted in Fig. 8. As in (II), an acid–base complex exhibiting an intermolecular O···H—N hydrogen bond between the carboxylic group and the pyridine ring is formed. These complexes are also linked by intermolecular OHO hydrogen bonds as in (II), exhibiting an O··· distance of 2.6996 (15) Å. The benzene ring in (IV) is almost coplanar with the carboxyl groups, because the nitro group in the *para*-position does not induce steric hindrance.

The two C—O distances of the carboxylic group of (IV) indicate a transfer of the proton in the intermolecular O···H—N hydrogen bond to nitrogen similar to that seen in (II). Again, the N···O distance is quite short [2.6122 (16) Å]. However, a big difference occurs in the intramolecular O···H—N hydrogen bond. The protonation of the pyridine ring leads to a shift of the proton in the intramolecular O···H—N hydrogen bond. In other words, the tautomeric equilibrium is shifted to the ketoamine form. This is manifested by a shortening of the C3′—O3′ distance of 1.2699 (17) and the increased N2—C4′ distance of 1.2919 (18) Å, that corresponds to an increased double-bond character of the first and an increased single-bond character of the second bond.

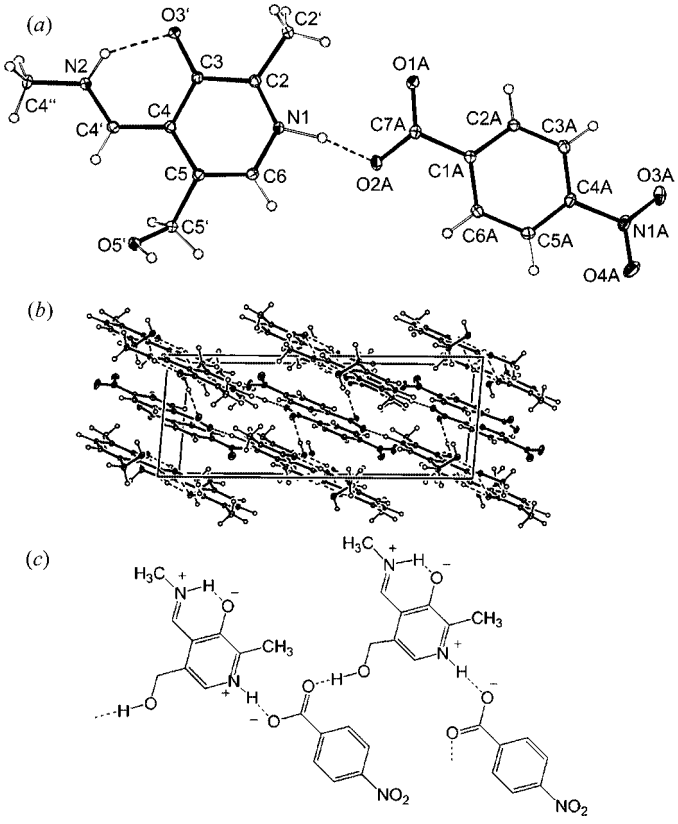

Figure 8
(*a*) X-ray crystal structure of (IV) showing the atom-numbering scheme. Displacement ellipsoids are drawn at the 30% probability level. (*b*) Crystal packing of (IV) along the *b* axis. (*c*) Showing schematically the stacking in columns of the pairs of molecules (IV) and the differences in the packing of these columns.

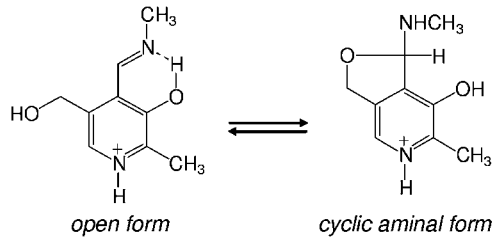

Figure 9
Equilibrium between the *open* and *cyclic aminal form.*

We also have studied the Schiff bases and their adducts (I)–(IV) with ^{1}H NMR in the liquid state. We note, however, that the NMR spectra of (I)–(IV) are complicated by the fact that in addition to the open form a *cyclic aminal* conformation can also be formed, depending on the solvent and the acid added (Fig. 9). For DMSO we find that the Schiff bases (I) and (III) are present in the *open form.*

This is in good agreement with earlier studies on pyridoximines (Harruff & Jenkins, 1976; van Genderen *et al.*, 1989). Furthermore, we observed that protonation of the ring N atom by dissolving the 1:1 adduct (IV) in DMSO resulted in the formation of the pyridinium salt of the *cyclic aminal* form; the H4′ resonance shifts upfield to 6.18 p.p.m. and the *N*-methyl signal was found at 2.37 p.p.m., as expected for an amine. For the *cyclic aminal form* of (IV) a ratio of 10% was found in the DMSO solution, estimated by integration of ^{1}H signals. A similar result was reported by van Genderen *et al.* (1989) who protonated (I) in DMSO with hydrochloride gas. By contrast, when the aldenamine adduct (II) was dissolved in DMSO, only the *open form* was observed.

4. Conclusions

Whenever the Schiff base N atoms of PLP carry an aliphatic substituent such as in the internal and external aldimines of PLP in the enzyme environment, protonation of the ring nitrogen will also shift the proton in the intramolecular OHN hydrogen bond from oxygen to the Schiff base nitrogen, a circumstance that increases its positive electric charge. This charge seems to be a pre-requisite for the reactivity of the enzyme. Finally, we note that this effect does not occur if the Schiff base N atom carries an aromatic substituent. In contrast, all crystallographic structures were observed in the *open form.* The protonation of the ring N atom of the acid–base adduct of the aldimine Schiff base in liquid state leads to the formation of the pyridinium salt of the *cyclic aminal* form.

S. Sharif and H.-H. Limbach wish to thank the Deutsche Forschungsgemeinschaft and the Fonds der Chemischen Industrie for financial support. D. R. Powell thanks the National Science Foundation (CHE-0079282) and the University of Kansas for funds to acquire the diffractometer and computers used in this work.

References

Benedict, C., Langer, U., Limbach, H.-H., Ogata, H. & Takeda, S. (1998). *Ber. Bunsenges. Phys. Chem.* **102**, 335–339.

Christen, P. & Metzler, D. E. (1985). Editors. *Tranaminases*. New York: Wiley.

Domiano, P., Musatti, A., Pelizzi, C. & Predieri, G. (1978). *Cryst. Struct. Commun.* **7**, 751–755.

Dziembowska, T., Rozwadowski, Z., Filarowski, A. & Hansen, P. E. (2001). *Magn. Reson. Chem.* **39**, 67–80.

Foces-Foces, C., Llamas-Saiz, A. L., Lorente, P., Golubev, N. S. & Limbach, H.-H. (1999). *Acta Cryst.* C**55**, 377–381.

Ferrari, M. B., Bisceglie, F., Leporati, E., Pelosi, G. & Tarasconi, P. (2002). *Bull. Chem. Soc. Jpn*, **75**, 781–788.

Fujiwara, T. (1973). *Bull. Chem. Soc. Jpn*, **46**, 863–871.

Genderen, M. H. P. van, van Lier, P. M. & Buck, H. M. (1989). *Recl. Trav. Chim. Pays-Bas*, **108**, 418–420.

Hansen, P. E., Sitkowski, J., Stefaniak, L., Rozwadowski, Z. & Dziembowska, T. (1998). *Ber. Bunsenges. Phys. Chem.* **102**, 410–413.

Harruff, R. C. & Jenkins, W. T. (1976). *Org. Mag. Reson.* **8**, 548–557.

Heyl, D., Luz, E., Harris, S. A. & Folkers, K. (1948). *J. Am. Chem. Soc.* **70**, 3669–3671.

Heyl, D., Luz, E., Harris, S. A. & Folkers, K. (1952). *J. Am. Chem. Soc.* **74**, 414–416.

Iwanami, M., Numata, T. & Murakami, M. (1968). *Bull. Chem. Soc. Jpn*, **41**, 161–165.

Jager, J., Moser, M., Sauder, U. & Jansonius, J. N. (1994). *J. Mol. Biol.* **239**, 285–305.

Jansonius, J. N. (1998). *Curr. Opin. Struct. Biol.* **8**, 759–769.

Kurahashi, M., Fukuoyo, M. & Shimada, A. (1967). *Bull. Chem. Soc. Jpn*, **40**, 1296.

Limbach, H.-H., Pietrzak, M., Sharif, S., Tolstoy, P. M., Shenderovich, I. G., Smirnov, S. N., Golubev, N. S. & Denisov, G. S. (2004). *Chem. Eur. J.* **10**, 5195–5204.

MacLaurin, C. L. & Richardson, M. F. (1985). *Acta Cryst.* C**41**, 261–263.

Malashkevich, V. N., Toney, M. D. & Jansonius, J. N. (1993). *Biochemistry*, **32**, 13451–13462.

Metzler, D. E. (1957). *J. Am. Chem. Soc.* **79**, 485–490.

Polanski, J. & Bak, A. (2003). *J. Chem. Info. Comput. Sci.* **43**, 2081–2092.

Rozwadowski, Z., Majewski, E., Dziembowska, T. & Hansen, P. E. (1999). *J. Chem. Soc. Perkin Trans. 2*, pp. 2809–2817.

Sakore, T. D. & Pant, L. M. (1966). *Acta Cryst.* **21**, 715–719.

Shaw, J. P., Petsko, G. A. & Ringe, D. (1997). *Biochemistry*, **36**, 1329–1342.

Sheldrick, G. M. (2000). *SHELXTL*, Version 6.10. Bruker AXS, Madison, Wisconsin, USA.

Sheldrick, G. M. (2002). *SADABS*. University of Göttingen, Germany.

Smith, D. L., Almo, S. C., Toney, M. D. & Ringe, D. (1989). *Biochemistry*, **28**, 8161–8167.

Souron, J.-P., Quarton, M., Robert, F., Lyubchova, A., Cosse-Barbi, A. & Doucet, J. P. (1995). *Acta Cryst.* C**51**, 2179–2182.

Spies, M. A. & Toney, M. D. (2003). *Biochemistry*, **42**, 5099–5107.

Stamper, C. G. F., Morollo, A. A. & Ringe, D. (1998). *Biochemistry*, **37**, 10438–10445.

Witherup, T. H. & Abbott, E. H. (1975). *J. Org. Chem.* **40**, 2229–2234.

Zhou, X. & Toney, M. D. (1999). *Biochemistry*, **38**, 311–320.